Original Article

Ferula sinkiangensis against gastric cancer: a network pharmacology, molecular docking and cell experiment study

Dexi Wang[1], Yun Sun[2], Qiaoyun Liu[1], Chenyu Ye[1], Shengjun Zhao[3,4], Haiying Zhang[3,4]

[1]Graduate School, the Fourth Clinical College of Xinjiang Medical University, Urumqi, China; [2]Department of Traditional Chinese Medicine, the Traditional Chinese Medicine College of Xinjiang Medical University, Urumqi, China; [3]Department of Pharmacy, Affiliated Hospital of Traditional Chinese Medicine of Xinjiang Medical University, Urumqi, China; [4]Xinjiang Key Laboratory of Processing and Research of Traditional Chinese Medicine, Urumqi, China

Contributions: (I) Conception and design: H Zhang; (II) Administrative support: S Zhao; (III) Provision of study materials or patients: H Zhang; (IV) Collection and assembly of data: D Wang; (V) Data analysis and interpretation: Y Sun; (VI) Manuscript writing: All authors; (VII) Final approval of manuscript: All authors.

Correspondence to: Shengjun Zhao, MD; Haiying Zhang, MD. Department of Pharmacy, Affiliated Hospital of Traditional Chinese Medicine of Xinjiang Medical University, No. 116, Huanghe Road, Sayibak District, Urumqi 830000, China. Email: 1519531677@qq.com; zzhhyy2583@126.com.

Background: *Ferula sinkiangensis* (*F. sinkiangensis*) is a traditional Chinese medicine that has been used for thousands of years to treat stomach ailments. To identify the main active compounds and explore the mechanisms underlying the therapeutic effect of *F. sinkiangensis* against gastric cancer (GC) by network pharmacology, molecular docking analysis and cell experiment.

Methods: Based on a review of the literature and previous experiments conducted by our research group, the active compounds of *F. sinkiangensis* were obtained. Active compounds and their target genes were screened from SwissADME, Pubchem, and Pharmmapper databases. GC-related target genes were obtained from GeneCards. The drug-compound-target-disease (D-C-T-D) network and protein-protein interaction (PPI) network were constructed by Cytoscape 3.7.2 and STRING database, and the core target genes and core active compounds were identified. Gene Ontology (GO) analysis and Kyoto Encyclopedia of Genes and Genomes (KEGG) pathway enrichment analysis were conducted using the R package clusterProfiler. The core genes with high expression in GC were screened, which correlated with a poor prognosis using the GEPIA, UALCAN, HPA, and KMplotter databases. KEGG signaling pathway analysis was further conducted to predict the mechanism of *F. sinkiangensis* during the process of GC inhibition. The AutoDock vina 1.1.2 program was used to verify the molecular docking of the core active compounds and core target genes. MTT, Transwell, and Wound healing assay were used to detect the effects of ethyl acetate extract of *F. sinkiangensis* on the proliferation, invasion, and apoptosis of GC cells.

Results: Final results indicated that the active compounds include Farnesiferol C, Assafoetidin, Lehmannolone, Badrakemone, etc. The identified core target genes were *GPI*, *TKT*, *GLYCTK*, *ERBB2*, *GAPDH*, etc. The Glycolysis/Gluconeogenesis pathway and the Pentose Phosphate pathway might play important roles in the treatment of GC with *F. sinkiangensis*. The data from the study showed that *F. sinkiangensis* was able to inhibit the proliferation of GC cells. Meanwhile, *F. sinkiangensis* remarkedly repressed the invasion and migration of GC cells in *in vitro* experiment.

Conclusions: This study revealed that *F. sinkiangensis* has an antitumor effect in in vitro experiment, and that the mechanism of *F. sinkiangensis* in GC treatment shows characteristics of multi-components, multi-targets, and multi-pathways, which provides a theoretical basis for its clinical application and subsequent experimental verification.

Keywords: *Ferula sinkiangensis (F. sinkiangensis)*; gastric cancer; network pharmacology; molecular docking; bioinformatics analysis; vitro experiment

Submitted Sep 26, 2022. Accepted for publication Mar 07, 2023. Published online Apr 28, 2023.
doi: 10.21037/tcr-22-2292
View this article at: https://dx.doi.org/10.21037/tcr-22-2292

Introduction

Gastric cancer (GC) is a malignant tumor threatening human health globally. According to the most recent statistics from the journal *CA: A Cancer Journal for Clinicians*, more than 1 million new cases of GC are reported every year. GC reportedly kills about 760,000 people annually and is the fourth most common types of cancer (1). GC morbidity and mortality rates in China are among the highest globally, accounting for roughly 40% of global GC cases (2). Notwithstanding that the past decade had witnessed significant inroads in surgical treatment, adjuvant radiotherapy, chemotherapy, and targeted therapy for GC patients, the 5-year survival rate for advanced GC has not improved significantly, reported to a range between 30% and 50% (3).

Ferula is a member of the Peucedanum family of Umbelliferae, with over 150 species found primarily in Central Asia, including Iran, Pakistan, Turkey, and the former Soviet Union. In China, 31 species are grown, with 25 species in the Xinjiang province. Ferula was first reported in the Newly Revised Materia Medica of the Tang Dynasty in China. According to the 2020 edition of the Chinese Pharmacopoeia, the resin of Ferula sinkiangensis (*F. sinkiangensis*) or Ferula fukanensis has the effect of eliminating food, removing blood stasis, dispersing a lump in the abdomen, and killing insects. An ancient saying goes as follows, "there is no fake in gold, and there is no truth in Ferula", implying that Ferula is difficult to come by and is regarded as a precious resource known as the "Gobi Treasure" and "National Treasure of Western Regions".

F. sinkiangensis is a traditional Chinese medicine used in China for thousands of years to treat stomach ailments. It has been documented in the Materia Medica of all dynasties. According to the Compendium of Materia Medica, "Ferula can eliminate meat accumulation and kill insects; therefore, it can detoxify and ward off evil spirits". *F. sinkiangensis* is classified as a dietary supplement or an insecticide. Xinjiang people have the habit of eating freshly grown leaves of *F. sinkiangensis*, which is believed to have the effects of invigorating the stomach, expelling parasites, and eliminating abdominal distension and abdominal pain. Over the past five years, research on the anticancer, anti-angiogenesis and P-glycoprotein inhibitor effects of Ferula has gained significant momentum, especially in Gharaei *et al.* reported that Ferula gummosa could inhibit proliferation and induce apoptosis on GC cell lines (4). Zhang *et al.* of the Chinese Academy of Medical Sciences reported that *F. sinkiangensis* could induce apoptosis and G0/G1 cycle arrest of GC cells, mediated by the Wnt signaling pathway (5,6). Over the years, our research group has published 21 papers on the antitumor and antioxidation properties of *F. sinkiangensis* since 2011 (7-10).

Network pharmacology is a new interdisciplinary field that uses a systematic network model to analyze the interaction between "traditional Chinese medicine compounds-disease-targets-pathways" and reveals the functioning mechanisms behind for drugs at the molecular level. It is now a comprehensive and effective method for conducting research on the pharmacological mechanisms of traditional Chinese medicine. At the moment, network pharmacology is constrained by various aspects of technology, such as limited information from the database, inability to accurately reflect the status of the patients, etc. However, as more researchers pay attention to network

Highlight box

Key findings

- This study showed that ethyl acetate extract of *F. sinkiangensis* weakened the proliferation, migration, and invasion of human gastric cancer SGC7901 cells, and systematically explained the potential mechanism of *F. sinkiangensis* in treating GC using network pharmacology.

What is known and what is new?

- Research on the anticancer inhibitor effects of Ferula has gained significant momentum.
- This study systematically explained the potential mechanism of *F. sinkiangensis* in treating GC using network pharmacology, molecular docking, and bioinformatics analysis technology for the first time.

What is the implication, and what should change now?

- In this study, the results are only predictions after all. And for the next step, we intend to use *F. sinkiangensis* to treat GC in both *in vivo* and *in vitro* experimental models, in order to analyze the express level of protein and the mRNA level by transcriptomics and proteomics studies.

pharmacology, the research of its related disciplines is also deepening, with growing number of data related to diseases and drugs, and the continuous improvement of computer technology and calculation and analysis software. Network pharmacology is anticipated to become more prevalent in the pharmacy industry in the coming years.

Herein, network pharmacology was used to predict the mechanism of *F. sinkiangensis*' antitumor activity on the biological, molecular level, and the findings were validated using molecular docking technology and bioinformatics analysis technology to provide the foothold for future studies for the development of pharmacodynamic materials based on its active compounds. We present the following article in accordance with the MDAR reporting checklist (available at https://tcr.amegroups.com/article/view/10.21037/tcr-22-2292/rc).

Methods

The study was conducted in accordance with the Declaration of Helsinki (as revised in 2013).

Active compounds and target genes prediction of F. sinkiangensis

The main chemical compounds of *F. sinkiangensis* were determined in a previous chemical compound separation experiment of *F. sinkiangensis* conducted by our research group and a literature review (11-18). The Simplified Molecular Input Line Entry System (SMILES) of chemical compounds was obtained from the PubChem database, and the active compounds of *F. sinkiangensis* were screened by the SwissADME database (19). Metabolites with high gastrointestinal absorption and at least two "YES" for Druglikeness indexes Lipinski, Ghose, Veber, Egan, and Muegge were selected in SwissADME. The potential target genes of each active compound were predicted with the help of the PharmMapper platform, and the target genes were screened with "NormFit" greater than 0.6 (20). The screened target genes were introduced into the Uniprot database to obtain the official gene name, and the predictive target genes of active compounds could be obtained after removing repetitive genes (21).

Collection of GC-related target genes

The relevant target genes were retrieved from the GeneCards database using the keyword "Gastric Cancer" and standardized by the Uniprot database (22). The genes obtained were GC's predictive target genes after excluding repetitive and false positive genes. If too many GC target genes are detected, those with a "Relevance Score" greater than 2 times the median were set as potential GC target genes.

Drug-Compound-Target-Disease (D-C-T-D) network construction

A Venn plot was generated to obtain the intersection of the predicted drug-related and disease-related target genes. Next, complex information networks were constructed based on the interactions of drugs (*F. sinkiangensis*), active compounds, intersected target genes, and disease (GC). Finally, Cytoscape 3.7.2 software was used to visualize and analyze the D-C-T-D network (23). The first five active compounds of degree were selected as the core active compounds.

Protein-protein interaction (PPI) network construction

The STRING online database was used to obtain PPI data of the previously overlapping targets in the network (24). The object was selected as "Homo sapiens," and confidence scores were greater than 0.900. An R package was used to screen the key targets with the top 30 degree values for visualization.

Gene Ontology (GO) and Kyoto Encyclopedia of Genes and Genomes (KEGG) pathway enrichment analyses

GO enrichment and KEGG pathway enrichment of the targets of *F. sinkiangensis* in the treatment of GC were analyzed using the R package clusterProfiler. After the screening, significantly enriched GO terms and KEGG signaling pathways with $P<0.05$ were chosen.

Expression of the core genes in stomach adenocarcinoma (STAD) and paracancerous gastric tissues

mRNA expression of core genes in STAD and paracancerous gastric tissues

STAD is a malignant neoplasm in the glandular epithelium of the stomach. The incidence of STAD accounts for 95% of malignant gastric tumors. According to KEGG enrichment pathway analyses, the mechanism of *F. sinkiangensis* in treating GC is related to the glycolysis/

gluconeogenesis, Pentose phosphate pathway and so on. Using GEPIA database, we analyzed the mRNA expression of seven core genes of PPI network related to energy metabolism in tumor cells (25). The target gene was entered, and the core target gene mRNA expression was obtained by clicking GEPIA after selecting the cancer species to be studied as STAD. The mRNA expression of the core target genes was analyzed using the UALCAN database (26). After the selection of the Cancer Genome Atlas (TCGA) module, the entering of the name of the core target gene, where "stomach adenocarcinoma" is selected, the mRNA expression data of the target gene in STAD could be obtained.

Immunohistochemical analysis of the core target genes in STAD and paracancerous gastric tissues

The Human Protein Atlas (HPA) database was retrieved for all core target genes whose mRNA were highly expressed in STAD (27). To obtain immunohistochemical results of the expression of the above target genes in stomach cancer tissues, "Stomach Cancer" during pathological analysis was chosen. "Stomach" was selected in the tissue option to obtain the immunohistochemical results of the above target genes in normal gastric tissue. ImageProPlus 6.0 was used to calculate the average optical density [AOD = integral optical density (IOD) sum/area sum]. The AOD of each pixel in the projected or cross-sectional image of the tested cell was referred to as AOD (28). In this study, AOD referred to the intracellular concentration of the measured protein and the staining depth.

Survival analysis of highly expressed core target genes in GC

KM plotter database includes 1,065 GC samples with follow-up data. The median overall survival (OS) was 28.9 months, and the median progression-free survival (PFS) was 18.3 months (29). The associations of the core genes verified by GEPIA, UALCAN, and HPA with survival rates of GC patients were explored by KM Plotter; the core genes for which higher expression indicated significantly worse survival were selected as potential immunotherapy biomarkers for GC. A P value <0.05 was statistically significant.

Molecular docking simulation

By docking the active compounds with the targets, the network pharmacology screening results were validated using the molecular docking software AutoDock 1.1.2 (Scripps Research, San Diego, CA, USA). Via computer simulations, small-molecule ligands were placed on the binding region of large-molecule receptors, and the physical and chemical parameters were calculated to predict the binding affinity. The gene crystal complexes of five PPI network core targets (*ERBB2*, *GAPDH*, *GPI*, *TKT*, *GLYCTK*) were downloaded in the PDB format from the RCSB PDB database, and PyMOL software (DeLano Scientific LLC, San Carlos, CA, USA) was used to remove water molecules and ligands (30). Through the use of the Chem3D software (Cambridgesoft Corporation, Cambridge, MA, USA), the sdf file of the core active compounds obtained from the PubChem database was converted into a mol 2 file with the lowest free energy. Finally, Ligands and receptors were processed with AutoDock Tools 1.5.6 and used AutoDock Vina 1.1.2 for molecular docking and analysis of docking results (31). PyMOL was used to visualize the results, and the hydrogen bonds and their binding sites were examined. The docking energy value was computed using the consistency score function of the ligand-receptor affinity (32). The affinity between the active compound and the related target was assessed by measuring the active compound's binding free energy to the target. The stronger the affinity, the lower the binding free energy required for docking.

Cell culture

SGC7901 cell lines (Shanghai Qingqi Biological Co., Ltd., China) were cultured in RPMI-1640 (Hyclone, Logan, UT, USA) (containing 10% fetal bovine serum, 100 U/mL penicillin, and 100 μg/mL streptomycin). All the cells were cultured in an incubator at 37 ℃ with 5% CO_2 and were subcultured after the cells grew to 70% to 80%. The cells used in the experiment were all logarithmic growth cells.

MTT assays

According to the standard of antineoplastic effect of natural drugs, the inhibition rate of plant crude extract on tumor cell IC_{50} less than 30 or 100 mg/L is about 80%, which can be preliminarily confirmed to have a certain anti-tumor effect. Therefore, SGC7901 cells were treated with five concentrations of ethyl acetate extract (250, 125, 62.5, 31.2 and 15.6 mg/L) from *F. sinkiangensis* for 48 hours. MTT

assays analyzed the proliferation of SGC7901 cells. About 2×10^5 cells were plated in 96-well plates and incubated for 24 hours. To assess cell viability, the cells were cultured with MTT solution (Solarbio, Beijing, China) (5 mg/mL) and incubated for 4 hours, and 150 µL DMSO (Sigma, St. Louis, MO, USA) was applied to treat the cells. The optical density value at 490 nm was detected with a microplate analyze (Thermo, Waltham, MA, USA).

Transwell assay

SGC7901 cells were seeded in a 6-well plate, and two concentrations (12.5, 6.25 mg/L) of ethyl acetate extract of *F. sinkiangensis* and positive control drug cisplatin (Jiangsu Hansoh Pharmaceutical Group Co., Ltd., Lianyungang, China) were added. After treatment for 48 hours, SGC7901 cells were collected, resuspended in serum-free cell culture medium, and were added to the upper chamber of the Transwell chamber (Corning, Corning, NY, USA). The chamber precoated with Matrigel (Corning) was used for the invasion assay and that without Matrigel was used for the migration assay. Cell culture medium containing 10% fetal bovine serum was added to the lower chamber. After culturing for 72 hours, the cells in the lower Transwell chamber were fixed with paraformaldehyde (4%) for 30 minutes and stained for 30 minutes. Finally, the number of migrated and invaded cells in each group was counted under the microscope.

Wound healing assay

SGC7901 cells were treated with ethyl acetate extract of *F. sinkiangensis* (12.5, 6.25 mg/L) and positive control drug cisplatin (12.5, 6.25 mg/L) for 48 hours. Approximately 2×10^5 SGC7901 cells were plated into the 24-well plates and incubated overnight to reach a fully confluent monolayer. A 20-µL pipette tip was applied to slowly cut a straight line across the well. The well was washed by phosphate buffered saline (PBS) three times and the medium was changed to serum-free medium and culture was continued. At 24 and 48 hours of incubation, the scratch distance (width between scratch lines) was measured, respectively. The wound healing percentage was calculated.

Statistical analysis

The SPSS17.0 statistical software (IBM, Armonk, NY, USA) was used, and the data are expressed as mean ± standard deviation (SD). One-way ANOVA was used for multiple comparisons followed by pairwise comparison with the least significant difference (LSD) method. A P value <0.05 indicates that the difference is statistically significant.

Results

Active compounds and target genes prediction of F. sinkiangensis

Based on our previous experiments on the separation of chemical compounds of *F. sinkiangensis* and a literature review, 56 main chemical compounds of *F. sinkiangensis* were identified. 23 active compounds of *F. sinkiangensis* were screened by SwissADME (*Table 1*). The potential target genes of 23 active compounds were predicted by the PharmMapper platform, and a total of 288 target genes were obtained by deleting repetitive values.

GC-related target genes

A total of 10,433 GC target genes were identified after removing repetitive and false positive genes from the GeneCards database and standardizing them with the Uniprot database. 2,727 GC target genes were screened based on the criteria "Relevance Score" greater than 2 times the median.

D-C-T-D network construction

By using Venny 2.1 to obtain the target gene set of GC and active compounds, 189 target genes were obtained (*Figure 1A*). Cytoscape 3.7.2 software was used to establish the D-C-T-D network, and the degree values of compounds-target genes were calculated, as shown in *Figure 1B*). The higher the degree, the closer the relationship between compounds and target genes, and the more important the compounds are in this network. According to the analysis of network topology parameters, active compounds with the first five of degree were screened as the core active compounds, and the five core active compounds are listed in *Table 2*.

PPI network analysis

To further explore the possible relationship between the intersected target genes and better understand the therapeutic mechanism of *F. sinkiangensis* for GC, we constructed a PPI network composed of 189 nodes and

Table 1 SwissADME screening of the active compounds of *F. sinkiangensis*

F. sinkiangensis compounds	Compound CID	GI absorption	Lipinski	Druglikeness	Bioavailability score
Asacoumarin B	4220856	High	Yes	4	0.56
Assafoetidin	131751454	High	Yes	5	0.55
Auraptene	1550607	High	Yes	4	0.55
Badrakemone	101793077	High	Yes	5	0.55
Diversin	13800313	High	Yes	5	0.55
Polyanthinin	7002233	High	Yes	2	0.55
Umbelliferone	5281426	High	Yes	3	0.55
Badrakemin	1771505	High	Yes	4	0.55
Farnesiferol B	1779468	High	Yes	4	0.55
Farnesiferol C	15559239	High	Yes	4	0.55
Farnesiferol A	7067262	High	Yes	5	0.55
Fekrynol acetate	59052606	High	Yes	2	0.55
Feshurin	11873225	High	Yes	5	0.55
Galbanic acid	11873225	High	Yes	4	0.56
Gummosin	7092581	High	Yes	5	0.55
Isofeterin	16093742	High	Yes	5	0.55
Isosamarcandin angelate	6442630	High	Yes	3	0.55
Lehmannolol	16093743	High	Yes	4	0.55
Lehmannolone	101418600	High	Yes	4	0.55
Karatavicinol	44386968	High	Yes	2	0.55
Methyl galbanate	7075765	High	Yes	4	0.55
Sinkianone	101418599	High	Yes	4	0.55
Ferulsinaic acid	102469382	High	Yes	4	0.56

GI, gastrointestinal.

130 edges, with an average connection degree of 1.38, as shown in *Figure 2A* and the top intersected 30 target genes are shown in *Figure 2B* and *Table 3*. The nodes represent the target genes, and the edges represent the relationship between proteins and proteins. In this PPI network, the degree of the target gene is proportional to its importance. As shown in *Figure 2B*, the target genes related to energy metabolism of tumor cells might be the key to the therapeutic effect of *F. sinkiangensis* against GC.

Go enrichment analysis

We used the clusterProfiler package to perform GO enrichment analysis on 29 target genes. Only GO terms with P<0.05 were significant, and the top GO 10 terms were visualized. A total of 474 items were significantly enriched in the biological process analysis, including response to steroid hormone, monosaccharide metabolic process, hexose metabolic process, multi-multicellular organism process, transcription initiation from RNA polymerase II promoter, pyridine nucleotide metabolic process, nicotinamide nucleotide metabolic process, female pregnancy, pyridine–containing compound metabolic process, and monosaccharide biosynthetic process (*Figure 3*).

For cellular component analysis, 37 items were enriched, including cell–cell junction, cytoplasmic vesicle lumen,

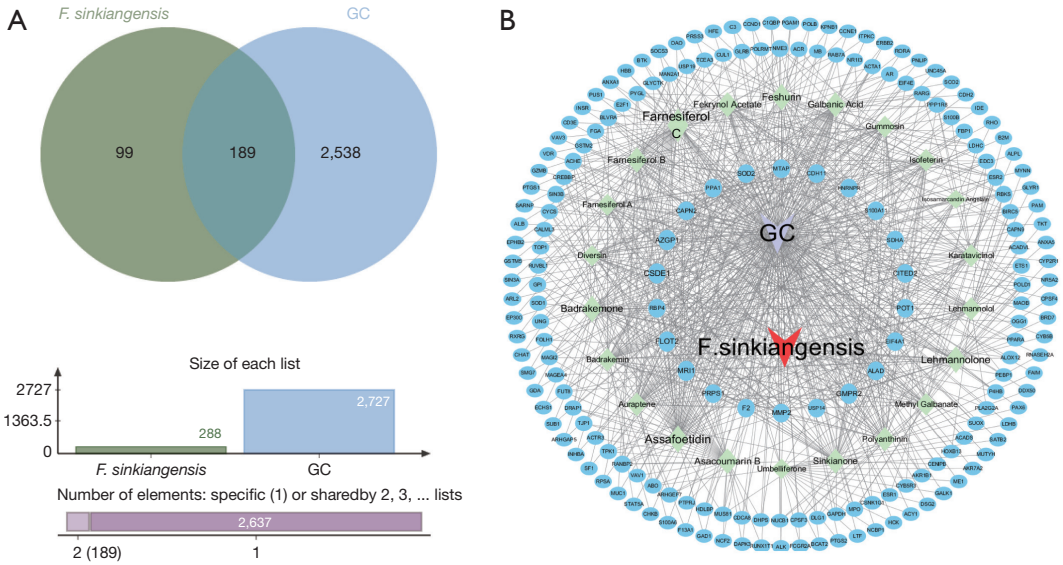

Figure 1 Venn diagram and D-C-T-D network. (A) Venn diagram. A total of 189 overlapping target genes between the disease and drug. (B) D-C-T-D network. The red arrow node represents the drug (*F. sinkiangensis*), the purple arrow node represents the disease (GC), 24 green rhombus nodes represent the active compounds in *F. sinkiangensis*, and 189 blue oval nodes represent the intersected target genes between *F. sinkiangensis* and GC. D-C-T-D, Drug-Compound-Target-Disease; GC, gastric cancer.

vesicle lumen, secretory granule lumen, transcription factor complex, nuclear chromatin, external side of the plasma membrane, membrane region, blood microparticle, and immunological synapse (*Figure 3*).

In terms of molecular function, 77 items were significantly enriched, including coenzyme binding, nuclear receptor activity, transcription factor activity, direct ligand regulated sequence–specific DNA binding, steroid hormone receptor activity, heme binding, tetrapyrrole binding, damaged DNA binding, antioxidant activity, hormone binding, and hydrolase activity, hydrolyzing N–glycosyl compounds (*Figure 3*).

KEGG enrichment analysis

The R package was used to perform KEGG enrichment analysis on 189 target genes. Only KEGG terms with P<0.05 were considered significant, yielding 104 relevant pathways. The top 15 KEGG pathways are displayed in *Table 4* and *Figure 4*. Significantly enriched pathways for *F. sinkiangensis* in GC included carbon metabolism, pentose phosphate pathway, chemical carcinogenesis-receptor activation, Glucagon signaling pathway, HIF-1 signaling pathway, glycolysis/gluconeogenesis, and biosynthesis of amino acids. These findings suggest that 7 energy metabolism-related pathways are significantly related to *F. sinkiangensis*'s anti-GC activity, implying that *F. sinkiangensis*'s therapeutic activity is mediated by inhibition of the tumor cell energy metabolism and promoting tumor cell apoptosis. According to KEGG enrichment pathway analyses, the mechanism of *F. sinkiangensis* in treating GC is related to the glycolysis/gluconeogenesis, pentose phosphate pathway, etc.

Expression of core genes before and after STAD

mRNA expression of core genes in STAD and paracancerous stomach tissues

Through the use of the GEPIA database, the TCGA analysis data of seven core genes were retrieved, and the mRNA expression data of core genes in STAD and paracancerous stomach tissues were studied. As shown in *Figure 5A*, six core genes *ERBB2*, *GAPDH*, *GPI*, *TKT*, *GLYCTK*, and *ME1* exhibited significantly higher mRNA levels in STAD tissues than in paracancerous stomach tissues (P<0.05). The mRNA expression of the six core genes was explored further by the UALCAN database. As shown in *Figure 5B*, except for *ME1*, the mRNA expression of the other five core genes was substantially higher in STAD tissues than in paracancerous stomach tissues by UALCAN (P<0.01). These

Table 2 The core compounds of *F. sinkiangensis*

No.	Core compounds	Degree	Molecular structure
01	Farnesiferol C	65	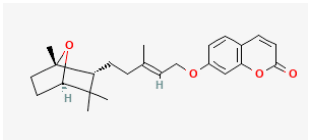
02	Assafoetidin	49	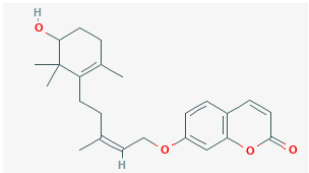
03	Lehmannolone	39	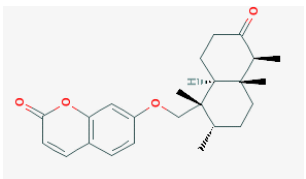
04	Badrakemone	38	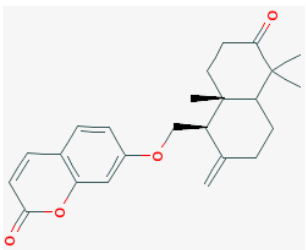
05	Feshurin	38	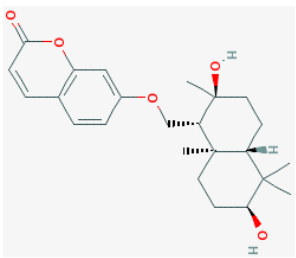

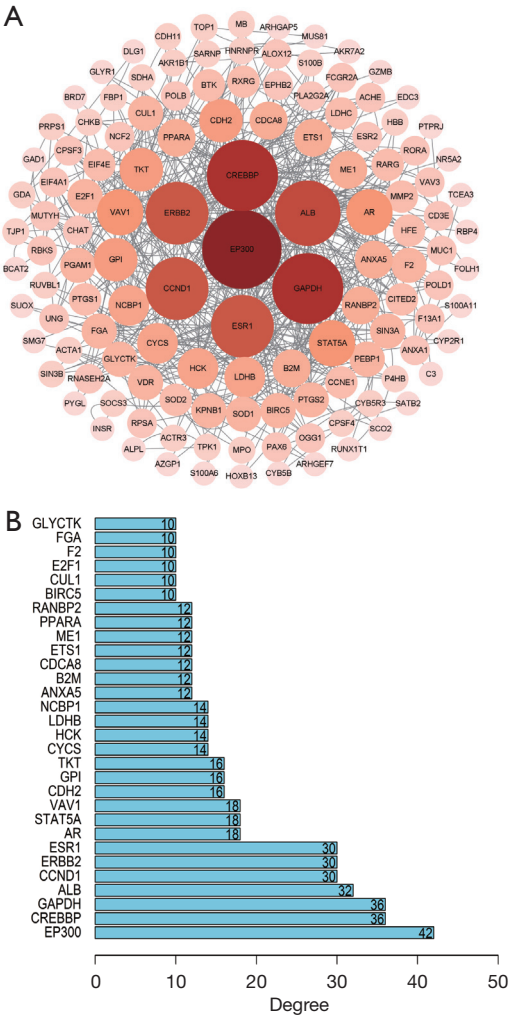

Figure 2 PPI network and core genes. (A) The PPI network. (B) The top 30 shared targets based on degree centrality. PPI, protein-protein interaction.

findings showed that the five core genes play a key role in the occurrence and progression of GC and are important target genes for GC diagnosis, intervention, and treatment.

Core target gene immunohistochemistry in STAD and paracancerous tissues

The HPA database was used to obtain immunohistochemical images of GPI, TKT, GLYCTK, ERBB2, and GAPDH in STAD and paracancerous stomach tissues, and the changes in protein expression in the core genes were analyzed. As shown in *Figure 6*, the findings revealed that the expression of these five core genes in STAD was significantly higher than in paracancerous stomach tissues at the protein level (P<0.01). Our findings suggested that the five core genes play a key role in the occurrence and progression of GC and are important target genes for GC diagnosis, intervention, and treatment.

Prognostic value of highly expressed core genes in GC

GPI, TKT, GLYCTK, ERBB2, and GAPDH expressions in GC patients were found in the database (*Figure 7*). From the survival curves, we found that high mRNA expression of GPI (HR: 1.79, 95% CI: 1.47–2.17, P=2e-09), TKT (HR: 2.48, 95% CI: 1.98–3.1, P=2.8e-16), ERBB2 (HR: 1.36, 95% CI: 1.13–1.64, P=0.0011), GAPDH (HR: 1.79, 95%

Table 3 Top 30 action target genes by degree

Target gene	Target protein	Degree
EP300	Histone acetyltransferase p300	42
CREBBP	CREB-binding protein	36
GAPDH	Glyceraldehyde-3-phosphate dehydrogenase	36
ALB	Serum albumin	32
CCND1	G1/S-specific cyclin-D1	30
ERBB2	Receptor tyrosine-protein kinase erbB-2	30
ESR1	Estrogen receptor	30
AR	Androgen receptor	18
STAT5A	Signal transducer and activator of transcription 5A	18
VAV1	Proto-oncogene vav	18
CDH2	Cadherin-2	16
GPI	Glucose-6-phosphate isomerase	16
TKT	Transketolase	16
CYCS	Cytochrome c	14
HCK	Tyrosine-protein kinase HCK	14
LDHB	L-lactate dehydrogenase B chain	14
NCBP1	Nuclear cap-binding protein subunit 1	14
ANXA5	Annexin A5	12
B2M	Beta-2-microglobulin	12
CDCA8	Borealin	12
ETS1	Protein C-ets-1	12
ME1	NADP-dependent malic enzyme	12
PPARA	Peroxisome proliferator-activated receptor alpha	12
RANBP2	E3 SUMO-protein ligase RanBP2	12
BIRC5	Baculoviral IAP repeat-containing protein 5	10
CUL1	Cullin-1	10
E2F1	Transcription factor E2F1	10
F2	Prothrombin	10
FGA	Fibrinogen alpha chain	10
GLYCTK	Glycerate kinase	10

CI: 1.49–2.14, P=1.7e-10), GLYCTK (HR: 1.26, 95% CI: 1.02–1.56, P=0.036) were associated with a poor prognosis.

Furthermore, our results showed that the overexpression of GPI (HR: 1.76, 95% CI: 1.44–2.15, P=2.9e-08), TKT (HR: 2.25, 95% CI: 1.79–2.84, P=2.1e-12), ERBB2 (HR: 1.27, 95% CI: 1.04–1.55, P=0.021), GAPDH (HR: 1.98, 95% CI: 1.62–2.42, P=1.6e-11) were related to poor FP (First Progression), whereas overexpression of GLYCTK (HR: 1.08, 95% CI: 0.85–1.38, P=0.5) was not related to FP. At the same time, the high expression of GPI (HR:

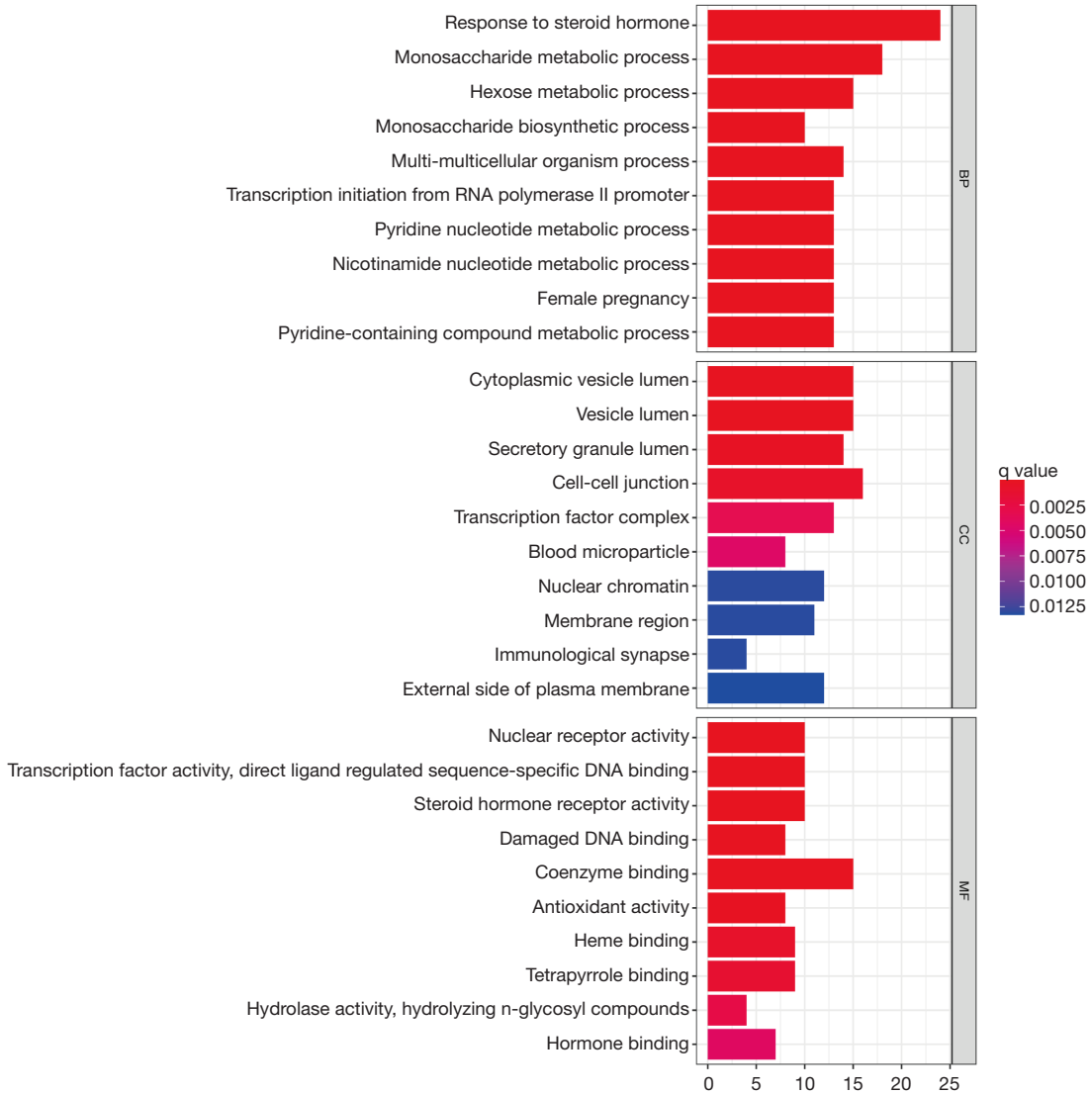

Figure 3 The results of GO enrichment analysis. The y-axis represents GO terms. The x-axis indicates the number of genes enriched (P<0.05). GO, Gene Ontology.

2.4, 95% CI: 1.92–3, P=3e-15), TKT (HR: 3.09, 95% CI: 2.44–3.92, P<1e-16), ERBB2 (HR: 1.65, 95% CI: 1.31–2.07, P=1.6e-05) and GAPDH (HR: 2.01, 95% CI: 1.61–2.51, P=3.8e-10), GLYCTK (HR: 1.78, 95% CI: 1.35–2.34, P=3.4e-05) were correlated with shorter post-progression survival (PPS).

In conclusion, this study provided novel insights into the role of GPI, TKT, GLYCTK, ERBB2, and GAPDH in GC and identified potential diagnostic and prognostic biomarkers. Indeed, GPI, TKT, GLYCTK, ERBB2, and GAPDH have huge prospects for application as immunotherapy biomarkers in GC patients.

Molecular docking simulation

The binding energy values were acquired using molecular docking studies. The docking details are provided in *Figure 8*, and the binding energies of the 5 core compounds in *F. sinkiangensis* with their core target genes were less than −5 kcal/mol, indicating high affinity; the less energy needed, the more stable the binding. To further study the interaction between compounds and target genes, the docking structure map and binding sites of each core compound and the target gene with the strongest affinity were visualized. As shown in *Figure 9*, the solid yellow line represents hydrogen bonding,

Table 4 KEGG pathway enrichment results

Pathway	Name	Number of target genes	p.adjust
hsa01200	Carbon metabolism	11	0.001054302
hsa00030	Pentose phosphate pathway	6	0.001288682
hsa05207	Chemical carcinogenesis-receptor activation	14	0.001331695
hsa04922	Glucagon signaling pathway	9	0.005706446
hsa03410	Base excision repair	5	0.011869038
hsa04066	HIF-1 signaling pathway	8	0.023980785
hsa05219	Bladder cancer	5	0.023980785
hsa00010	Glycolysis/gluconeogenesis	6	0.03218902
hsa04520	Adherens junction	6	0.03227022
hsa05215	Prostate cancer	7	0.03227022
hsa05223	Non-small cell lung cancer	6	0.03227022
hsa05166	Human T-cell leukemia virus 1 infection	11	0.03227022
hsa00270	Cysteine and methionine metabolism	5	0.03227022
hsa01230	Biosynthesis of amino acids	6	0.033186575
hsa00640	Propanoate metabolism	4	0.036450369

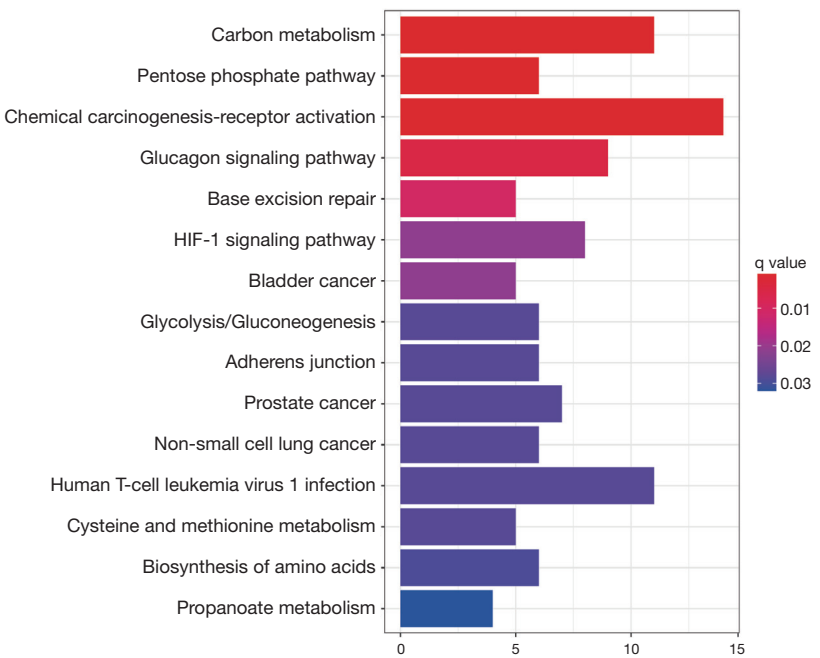

Figure 4 KEGG pathway enrichment analysis. The x-axis represents the counts of the target symbols in each pathway; the y-axis represents the main pathways (P<0.01). KEGG, Kyoto Encyclopedia of Genes and Genomes.

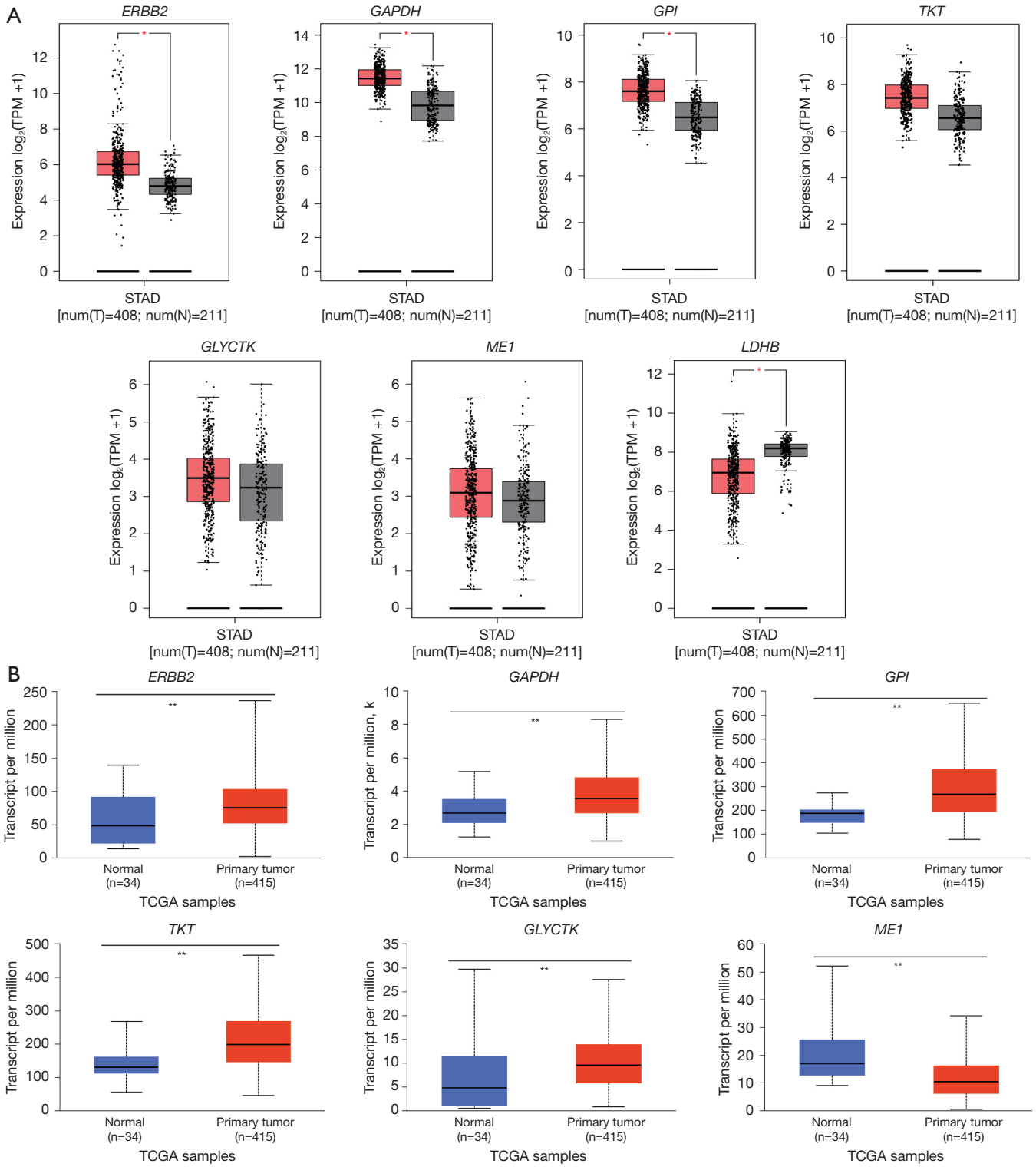

Figure 5 Expression level of core targets. (A) Except for *LDHB*, the mRNA expression of the other six core genes expressed much higher in STAD than in normal gastric tissues by GEPIA (*, P<0.05). (B) Except for *ME1*, the mRNA expression of the other five core genes was substantially higher in STAD tissues than in paracancerous stomach tissues by UALCAN (**, P<0.01). TPM, transcripts per million; STAD, stomach adenocarcinoma; TCGA, The Cancer Genome Atlas.

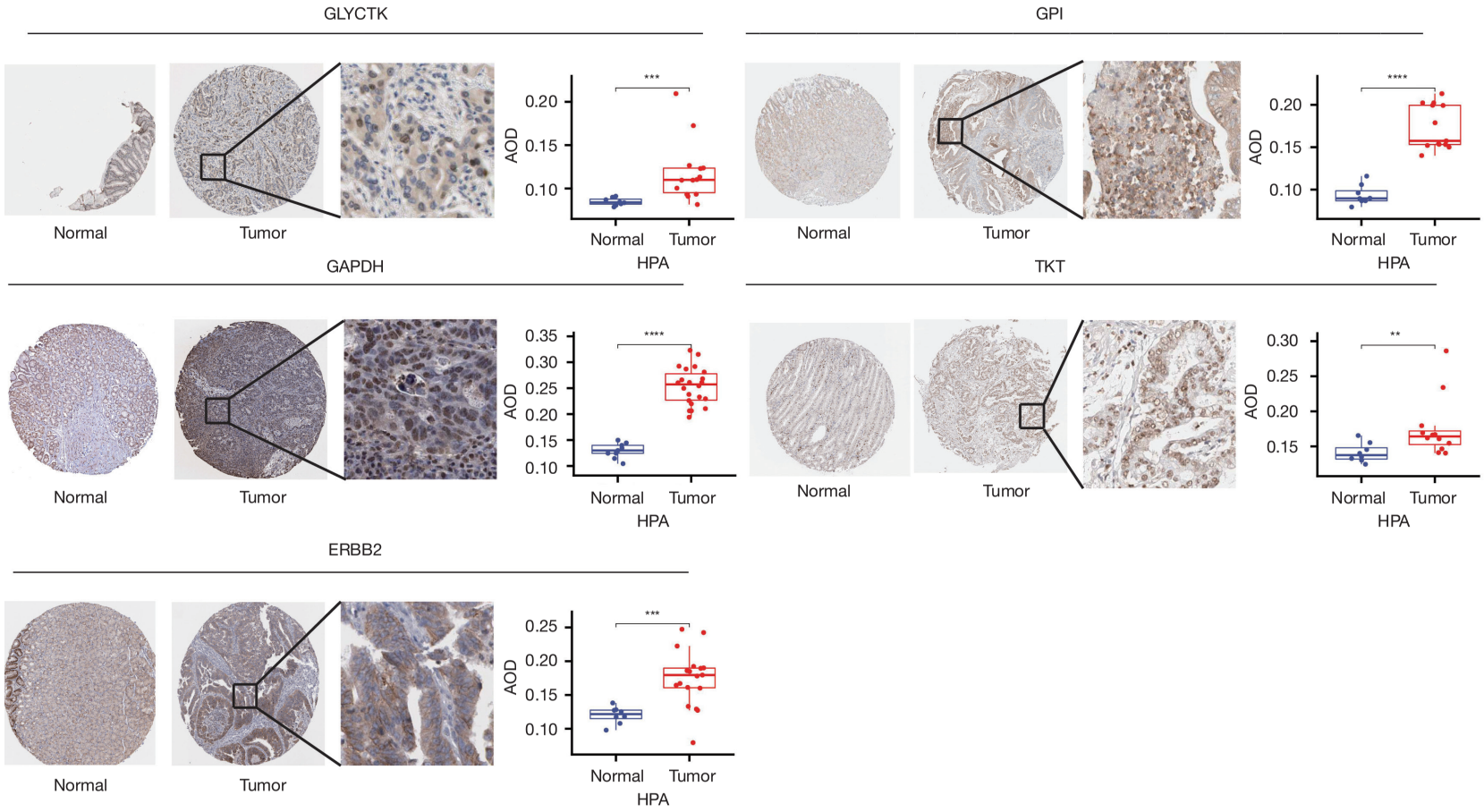

Figure 6 AOD results show that the expression of these five core genes in STAD was significantly higher than in paracancerous stomach tissues at the protein level via HPA (**P<0.01). GLYCTK, normal sample (image available from https://www.proteinatlas.org/ENSG00000168237-GLYCTK/tissue/stomach#img). GLYCTK, tumor sample (image available from https://www.proteinatlas.org/ENSG00000168237-GLYCTK/Pathology/stomach+Cancer#img). GPI, normal sample (image available from https://www.proteinatlas.org/ENSG00000105220-GPI/tissue/stomach#img). GPI, tumor sample (image available from https://www.proteinatlas.org/ENSG00000105220-GPI/pathology/stomach+cancer#img). GAPDH, normal sample (image available from https://www. proteinatlas.org/E NSG00000111640-GAPDH/tissue/stomach#img). GAPDH, tumor sample (image available from https://www.proteinatlas.org/ENSG00000111640-GAPDH/pathology/stomach+cancer#img). TKT normal sample, (image available from https://www.proteinatlas.org/ENSG00000163931-TKT/tissue/stomach#img). TKT tumor sample (image available from https://www.proteinatlas.org/ENSG00000163931-TKT/pathology/stomach+cancer#img). ERBB2 normal sample (image available from https://www.proteinatlas.org/ENSG00000141736-ERBB2/tissue/stomach#img). ERBB2 tumor sample (image available from https://www.proteinatlas.org/ENSG00000141736-ERBB2/pathology/stomach+cancer#img). **, P<0.01; ***, P<0.001; ****, P<0.0001. AOD, average optical density; STAD, stomach adenocarcinoma; HPA, Human Protein Atlas.

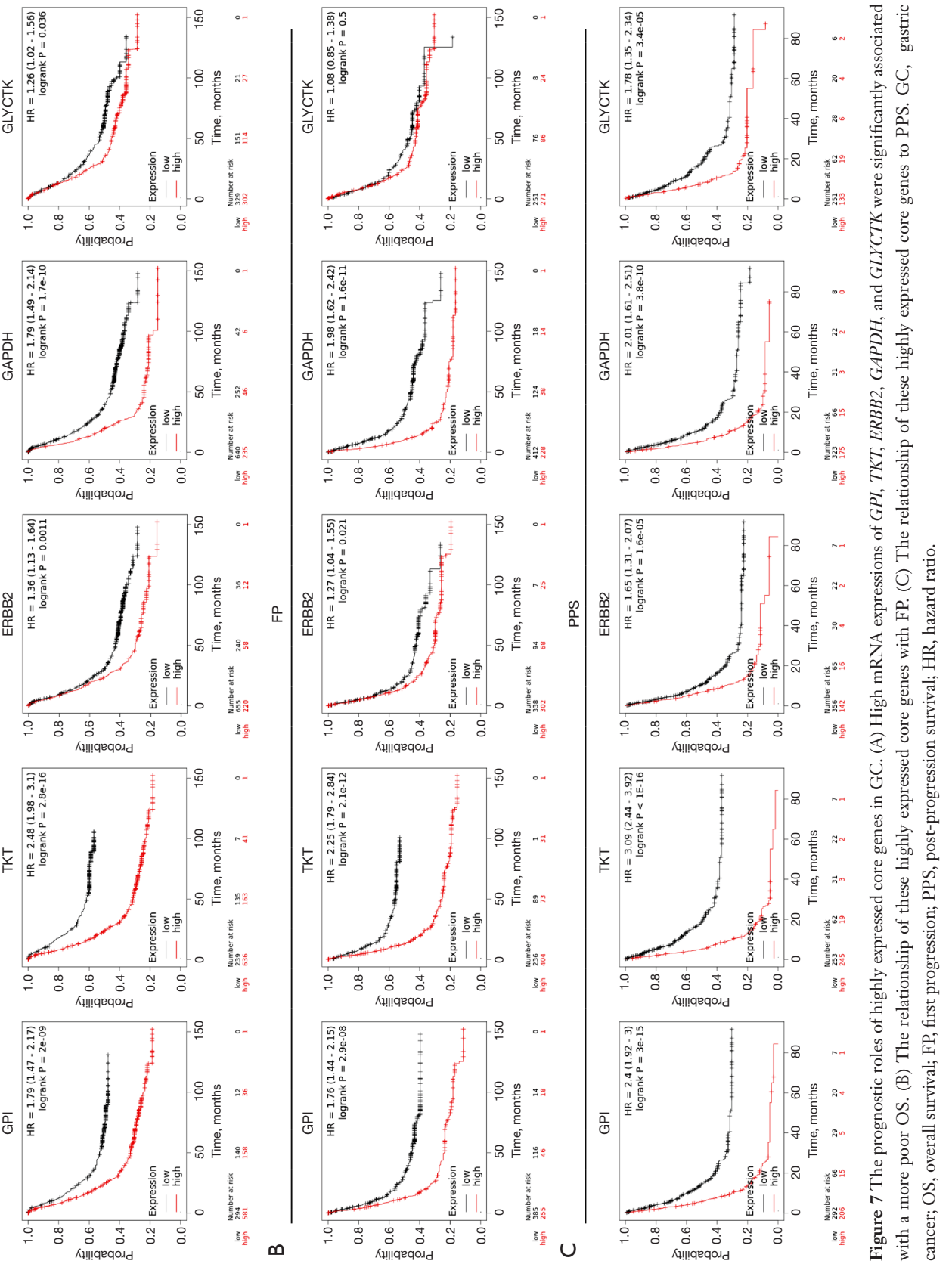

Figure 7 The prognostic roles of highly expressed core genes in GC. (A) High mRNA expressions of *GPI*, *TKT*, *ERBB2*, *GAPDH*, and *GLYCTK* were significantly associated with a more poor OS. (B) The relationship of these highly expressed core genes with FP. (C) The relationship of these highly expressed core genes to PPS. GC, gastric cancer; OS, overall survival; FP, first progression; PPS, post-progression survival; HR, hazard ratio.

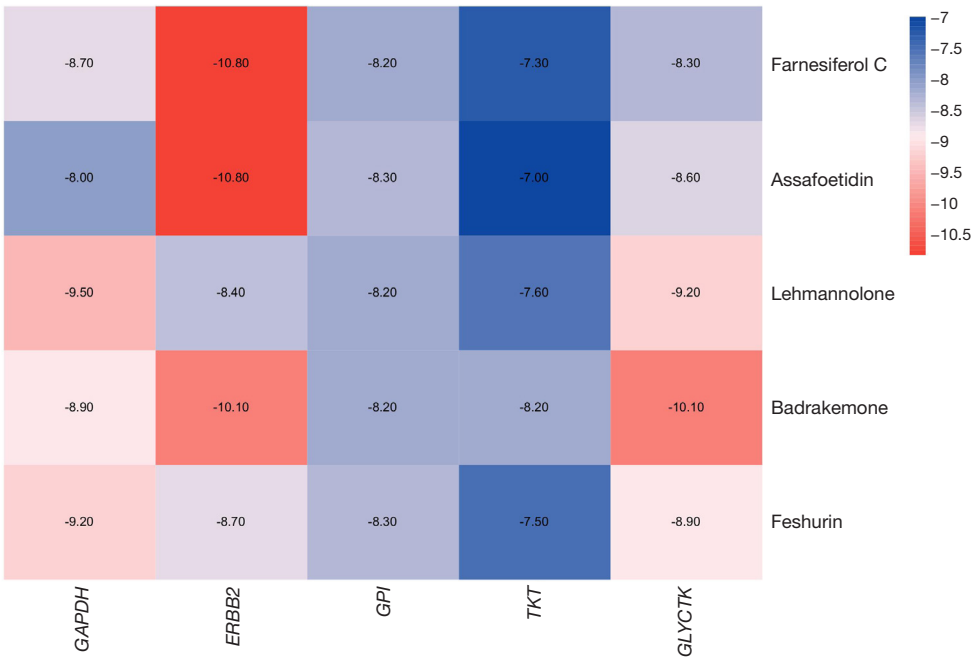

Figure 8 Docking score of core active compounds of *F. sinkiangensis* with core target genes.

and the dotted line represents hydrophobic interactions. Fewer amino acid residues were observed around the compound, mainly bound to the compound by electrostatic (hydrogen bonding) and hydrophobic interactions. The results of molecular docking revealed that Farnesiferol C, Assafoetidin, Lehmannolone, Badrakemone, and Feshurin were the main compounds of *F. sinkiangensis* in the treatment of GC.

Ethyl acetate extract of F. sinkiangensis decreases proliferation of GC cells

The MTT assay was performed to analyze cell proliferation. Ethyl acetate extract of *F. sinkiangensis* repressed the viability of SGC7901 cells in a dose-dependent manner and 250 mg/L *F. sinkiangensis* extract had a greater effect. As shown in *Figure 10*, *F. sinkiangensis* extract (125, 250 mg/L) markedly reduced proliferation of SGC7901 cells, suggesting that *F. sinkiangensis* extract decreases proliferation of GC cells.

Ethyl acetate extract of F. sinkiangensis reduces invasion and migration of GC cells

We further measured the effect of ethyl acetate extract of *F. sinkiangensis* on the migration and invasion of GC cells. As shown in *Figure 11A*,*11B*, transwell assays indicated that the migration and invasion of SGC7901 cells were markedly decreased by *F. sinkiangensis* extract (6.25, 12.5 mg/L). Consistently, the treatment of *F. sinkiangensis* extract (6.25, 12.5 mg/L) significantly repressed wound healing in SGC7901 cells (*Figure 11C*), indicating that *F. sinkiangensis* extract is able to attenuate the migration and invasion of GC cells.

Discussion

In this study, *F. sinkiangensis* was found to have an antitumor effect in *in vitro* models, inhibiting the proliferation, migration, and invasion of GC cells, corroborating that *F. sinkiangensis* has a clear anti-GC effect and is worth further research and development.

The material basis and mechanism of *F. sinkiangensis* in the treatment of GC were investigated using network pharmacology and molecular docking techniques in this study. 23 putative active compounds and 189 related target genes were screened. When the drug-compound-target-disease network was established, 5 core active compounds of *F. sinkiangensis* in treating GC were identified, including Assafoetidin, Badrakemone, Farnesiferol C, Feshurin, Lehmannolone. These 5 active ingredients were Ferula-specific sesquiterpenes and coumarins. These chemical

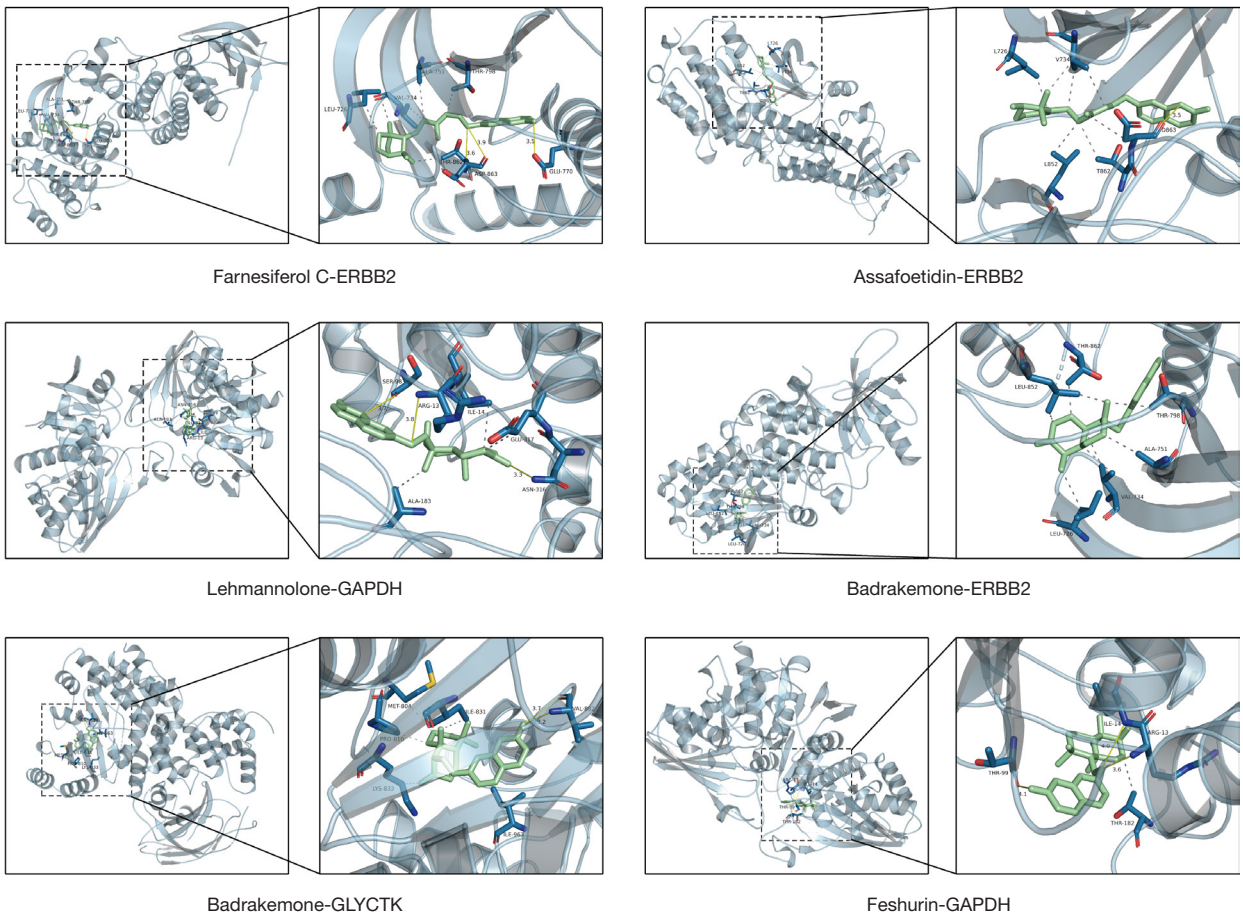

Figure 9 The model of molecular docking. The solid yellow line represents hydrogen bonding, and the dotted line represents hydrophobic interactions; these amino acid residues are mainly bound to the compound by electrostatic (hydrogen bonding) and hydrophobic interactions.

compounds have been associated with many properties, including anticancer, P-glycoprotein inhibition, and antiinflammation. Kasaian *et al.* reported that Farnesiferol A, B, and C have tumor cytotoxicity, apoptosis promotion, reversal of multidrug resistance, and antimutagenic activity (33-35). Hasanzadeh *et al.* discovered that in the MCF-7 cell line, farnesiferol C causes cell cycle arrest and apoptosis that is mediated by oxidative stress (36). Li *et al.* discovered that chemicals extracted from the seeds of *F. sinkiangensis*, such as Lehmannolone, Lehmannolol, Sinkianone, and Fekrynol, inhibits the growth of cervical cancer HeLa cells, with IC_{50} values ranging from 20.4 to 226.2 μmol.L^{-1} (37). Kamoldinov *et al.* reported that Feshurin showed high inhibitory activity against mino human lymphocyte cell with IC_{50} values of 7.88±0.60 μM (38). In non-small-cell lung cancers (NSCLCs), Jung JH found that Farnesiferol C increases the antitumor effects of puromycin or doxorubicin and induces apoptosis and G1 arrest through the regulation of ribosomal protein L11 and c-Myc (39).

PPI network analysis of the key target genes of *F. sinkiangensis* in anti-GC showed significant enrichment in biological processes such as glycolysis metabolism and Pentose phosphate pathway. 15 signaling pathways significantly related to the treatment of GC by *F. sinkiangensis* were screened using GO and KEGG pathway enrichment analyses with P<0.05 as the criteria, including the glycolysis/gluconeogenesis, glucagon signaling pathway, carbon metabolism, pentose phosphate pathway, cysteine and methionine metabolism, HIF-1 signaling pathway, biosynthesis of amino acids, propanoate metabolism, chemical carcinogenesis-receptor activation, base excision repair, bladder cancer, adherens junction, prostate cancer, NSCLC, human T-cell leukemia virus 1 infection. These findings suggest that 7 energy metabolism-

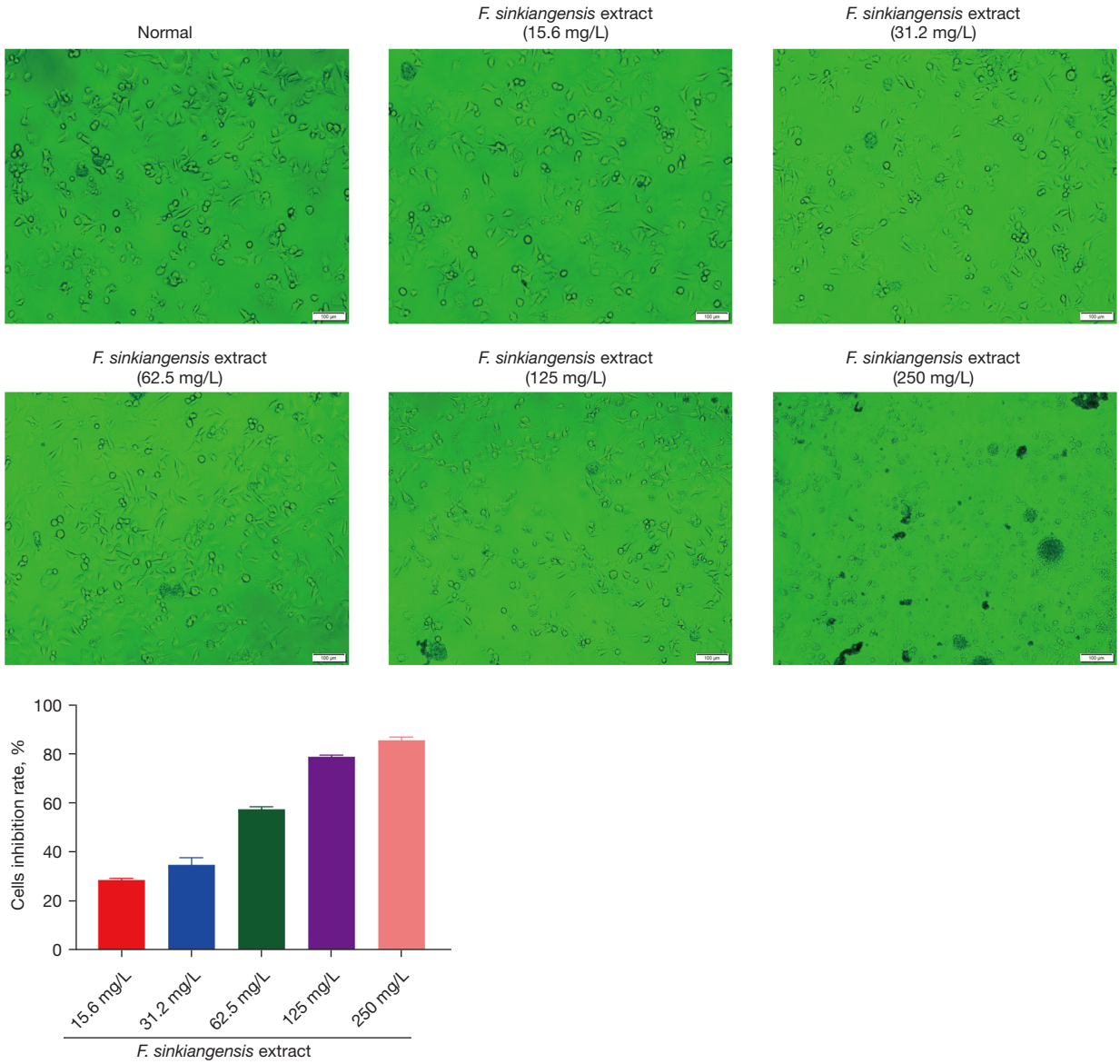

Figure 10 The MTT assay was performed to analyze cell proliferation. The inhibition of proliferation of SGC7901 cells by ethyl acetate extract of *F. sinkiangensis*. *F. sinkiangensis* extract (15.6, 31.2, 62.5, 125, and 250 mg/L) was used to treat SGC7901 cells. MTT, methyl thiazolyl tetrazolium.

related pathways are significantly related to *F. sinkiangensis*'s anti-GC activity, implying that *F. sinkiangensis*'s therapeutic activity is mediated by inhibition of the tumor cell energy metabolism and promoting tumor cell apoptosis. According to KEGG enrichment pathway analyses, the mechanism of *F. sinkiangensis* in treating GC is related to the glycolysis/gluconeogenesis, pentose phosphate pathway and so on.

OttoWarburg, Nobel Laureate in Physiology or Medicine, identified aberrant energy metabolism in cancer in 1931. Interestingly, even in the presence of plentiful oxygen, adenosinetriphosphate (ATP) synthesis in tumor cells does not result from oxidative phosphorylation of glucose but rather with a faster glycolysis rate, increasing the glucose intake and the lactic acid formation, which is called aerobic glycolysis, or the Warburg effect. One of the most basic characteristics of malignancies is the Warburg effect. It is widely acknowledged that high-rate glycolysis is the primary source of energy for rapidly growing tumor

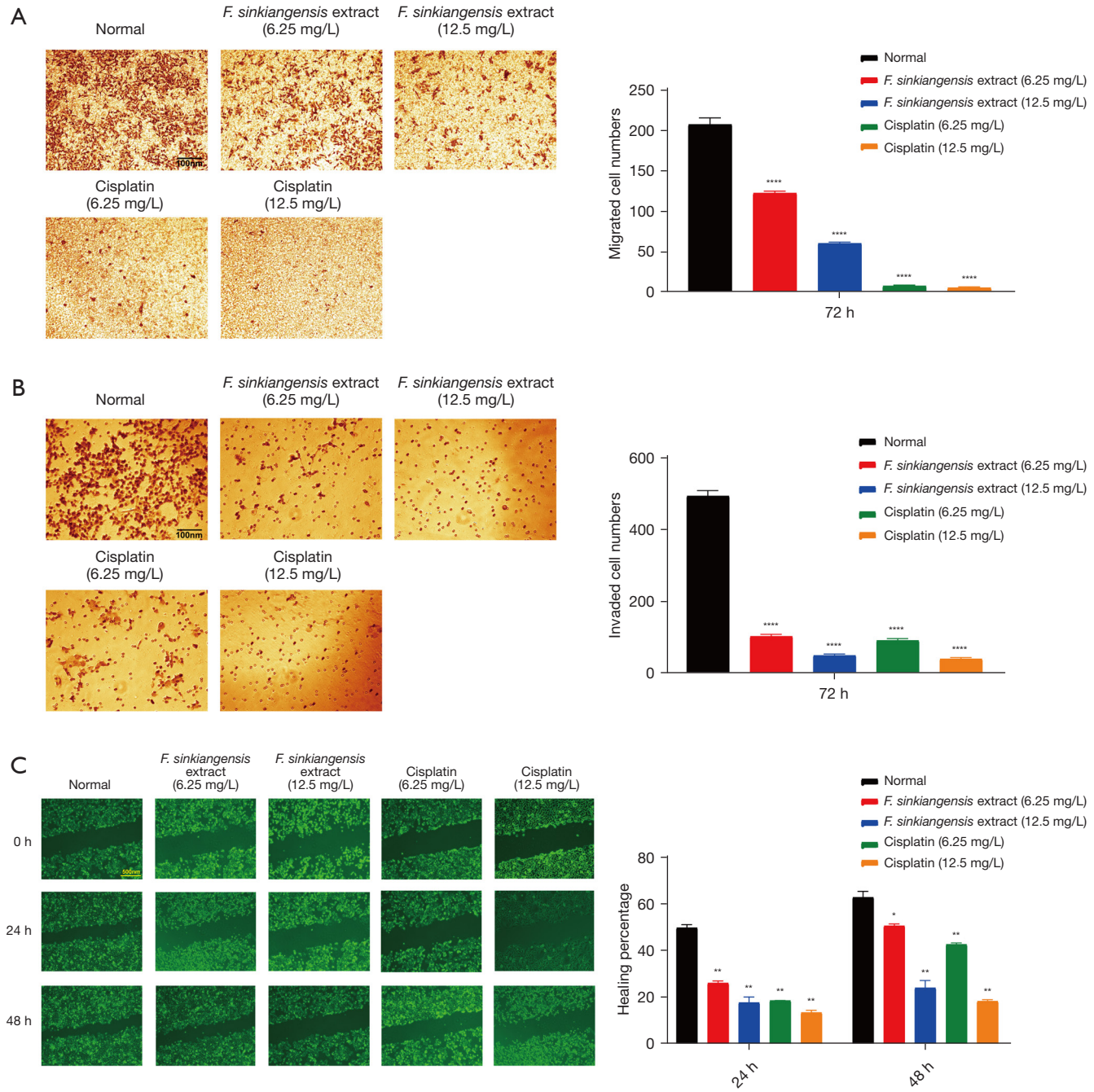

Figure 11 Ethyl acetate extract of *F. sinkiangensis* reduces invasion and migration of gastric cancer cells. (A,B) Transwell assays analyzed migrated and invaded cell numbers, ****, P<0.0001 compared with normal control. Cells were fixed with paraformaldehyde and stained with crystal violet. (C) Wound healing assays examined migration and invasion. The wound healing percentage is shown. *P<0.05, **, P<0.01 compared with normal control.

cells, which enhances tumor adaptability to hypoxia and other stressful environments and boosts the malignant potential of tumors (40). In recent years, tumor research has shifted its focus to targeted aerobic glycolysis.

In the glycolysis/gluconeogenesis process, *F. sinkiangensis* inhibited the activity of six related enzymes, indicating its importance. Glycolysis involves the breaking down of glucose or glycogen into pyruvate in the cytoplasm without using oxygen and generating tiny amounts of ATP. Even when there is enough oxygen, ATP generation in tumor tissue comes from aerobic glycolysis, known as the Warburg effect. In this study, GPI can transform glucose-6-phosphate and fructose-6-phosphate into each other in the cytoplasm. Fructose-1,6-bisphosphatase 1 (FBP1) catalyzes the conversion of fructose-6-phosphate to fructose-1,6-diphosphate. GAPDH catalyzes the conversion of glyceraldehyde 3-phosphate to 1,3-diphosphoglyceric acid. Phosphoglycerate dismutase (PGAM) catalyzes 3-phospho-D-glyceric acid rearrangement to form 2-phosphoglyceric acid. It has been established that tumor cells rely on lactate dehydrogenase (LDHB) to produce lactic acid after glucose is metabolized to pyruvate by glycolysis, which alters the tumor cell microenvironment and aids tumor cell invasion, metastasis, and immune evasion (41). ErbB2 is a transmembrane receptor tyrosine kinase that governs cell physiological responses such as cell growth, division, differentiation, adhesion, function, and apoptosis. ErbB2 promoted glycolysis via heat shock factor 1 (HSF1)/lactate dehydrogenase A (LDHA) axis and ErbB2-mediated glycolysis was required for the growth of breast cancer cells (42).

The pentose phosphate pathway (PPP), which branches from glycolysis at the first committed step of glucose metabolism, is required for the synthesis of ribonucleotides and is a major source of NADPH (43). By providing cells with both ribose-5-phosphate and NADPH for the detoxification of intracellular reactive oxygen species, reductive biosynthesis, and ribose biogenesis, PPP plays a crucial role in controlling the growth of cancer cells. As a result, changes to the PPP directly affect cell growth, survival, and senescence (44).

In the PPP, it appears that *F. sinkiangensis* works by inhibiting the activity of three related enzymes. To meet the unlimited and exuberant growth needs of tumor cells, the metabolic pentose phosphate pathway, which is rarely used in normal cells, is activated in tumor cells. In this study, transketolase (TKT) was found to be a rate-limiting enzyme in the non-oxidative part of the PPP that is responsible for maintaining ribose 5-phosphate levels. For cell proliferation to continue, TKT is required (45,46). Ribose-phosphate pyrophosphokinase 1 (PRPS1) and ribokinase (RBKS) are involved in nucleotide biosynthesis and subsequent purine and pyrimidine biosynthesis (47).

Herein, bioinformatics analysis was used to confirm the five core target genes: *GPI*, *TKT*, *GLYCTK*, *ERBB2*, and *GAPDH*. The five core target genes were highly expressed in GC tissues, which were potential biomarkers for the diagnosis and prognosis of GC and played an important role in the pathogenesis and treatment of GC, according to mRNA, protein expression, and survival time. Using molecular docking, the five active compounds were tightly correlated to GC-related core target genes. These findings demonstrate that *F. sinkiangensis* may inhibit GC cells from metabolizing energy, such as glycolysis and pentose phosphate pathways, by suppressing the expression of the *GPI*, *TKT*, *GLYCTK*, *ERBB2* and *GAPDH* genes. This would inhibit GC cells from proliferating, migrating, and invading healthy tissue.

In this study, although the possible targets by *F. sinkiangensis* on GC was predicted with network pharmacology and molecular docking, the results are only predictions after all. And for the next step, we intend to use *F. sinkiangensis* to treat GC in both *in vivo* and *in vitro* experimental models, in order to analyze the express level of protein and the mRNA level by transcriptomics and proteomics studies.

Conclusions

To summarize, this study showed that ethyl acetate extract of *F. sinkiangensis* weakened the proliferation, migration, and invasion of human gastric cancer SGC7901 cells, and systematically explained the potential mechanism of *F. sinkiangensis* in treating GC using network pharmacology, molecular docking, and bioinformatics analysis technology. Assafoetidin, Badrakemone, Farnesiferol C, Feshurin, Lehmannolone, and other sesquiterpenes and coumarins are found to be the main active ingredients. *F. sinkiangensis* promotes tumor cell apoptosis and prevents energy metabolism by inhibiting the glycolysis/gluconeogenesis and pentose phosphate pathways. This study aims to provide the foothold for further studies on the pharmacodynamics of *F. sinkiangensis* and new ideas for improving the application of traditional Chinese medicine in treating GC. However, further studies are warranted to validate the putative mechanisms revealed by this research.

Acknowledgments

Funding: The work was supported by the National Natural Science Foundation of China (Grant No. 82060734) and Natural Science Foundation of Xinjiang Uygur Autonomous Region (Grant No. 2020D01C144).

Footnote

Reporting Checklist: The authors have completed the MDAR reporting checklist. Available at https://tcr.amegroups.com/article/view/10.21037/tcr-22-2292/rc

Conflicts of Interest: All authors have completed the ICMJE uniform disclosure form (available at https://tcr.amegroups.com/article/view/10.21037/tcr-22-2292/coif). The authors have no conflicts of interest to declare.

Ethical Statement: The authors are accountable for all aspects of the work in ensuring that questions related to the accuracy or integrity of any part of the work are appropriately investigated and resolved. This study was conducted in accordance with the Declaration of Helsinki (as revised in 2013).

References

1. Sung H, Ferlay J, Siegel RL, et al. Global Cancer Statistics 2020: GLOBOCAN Estimates of Incidence and Mortality Worldwide for 36 Cancers in 185 Countries. CA Cancer J Clin 2021;71:209-49.
2. Global, regional, and national age-sex-specific mortality for 282 causes of death in 195 countries and territories, 1980-2017: a systematic analysis for the Global Burden of Disease Study 2017. Lancet 2018;392:1736-88.
3. Eusebi LH, Telese A, Marasco G, et al. Gastric cancer prevention strategies: A global perspective. J Gastroenterol Hepatol 2020;35:1495-502.
4. Gharaei R, Akrami H, Heidari S, et al. The suppression effect of Ferula gummosa Boiss. extracts on cell proliferation through apoptosis induction in gastric cancer cell line. Eur J Integr Med 2013;5:241-7.
5. Zhang L, Si J, Li G, et al. Umbelliprenin and lariciresinol isolated from a long-term-used herb medicine Ferula sinkiangensis induce apoptosis and G0/G1 arresting in gastric cancer cells. RSC Adv 2015;5:91006-17.
6. Zhang L, Sun X, Si J, et al. Umbelliprenin isolated from Ferula sinkiangensis inhibits tumor growth and migration through the disturbance of Wnt signaling pathway in gastric cancer. PLoS One 2019;14:e0207169.
7. Yan L, Zhao S, Zhang H, et al. Effects of five kinds of Resina Ferulae in Xinjiang on cell proliferation inhibition and apoptosis of human gastric carcinoma SGC-7901 cells in vitro. China Journal of Traditional Chinese Medicine and Pharmacy 2020;35:5486-90.
8. Zhang H, Li W, Zhou L, et al. Screening of Active Parts of Xinjiang Ferulae Resina with Anti-tumor Effects. Chinese Journal of Information on Traditional Chinese Medicine 2016;23:52-6.
9. Luo F, Lu J, Zhang H, et al. Inhibitory Effect of Ethyl Acetate Part of Ferula sinkiangensis on S180 Solid Tumor in Mice. China Pharmacy 2016;27:4388-91.
10. Yan L, Li W, Zhao S, et al. Study on GC-MS fingerprint of volatile oil from Ferula Soongarica and its anti-gastric cancer effect. Journal of Xinjiang Medical University 2020;43:957-61.
11. Mei L, Wang X, Wang Y. Research Progress on Chemical constituents, Pharmacological Action and Toxicology of Ferula officinalis. China Pharmacy 2016;27:534-8.
12. Wang L, Sun R, Xu M, et al. Research on the Development of Chemical Components, Pharmacological Activities and Toxicity of Resina Ferulae. World Chinese Medicine 2020;15:3887-94.
13. Yang X. Bioactive Material Basis of Medicinal Plants in Genus Ferula. Modern Chinese Medicine 2018;20:123-44.
14. Xing Y, Li N, Xue J, et al. Research Progress on Chemical constituents of Ferula. Journal of Shenyang Pharmaceutical University 2012;29:730-41.
15. Patiguli F, Xieraili T, Gulishan M, et al. Clinical Application and Research Progress of Uighur Medicine Ferula in Uygur Medicine. Journal of Medicine and Pharmacy of Chinese Minorities 2011;17:61-4.
16. Huang Y, Yue L, Shen X, et al. Chemical constituents and pharmacological activities of Ferula sinkiangensis K.M.Shen: research advances. Journal of International

Pharmaceutical Research 2017;44:495-9.
17. Zhao B, Gui H, Zhu Y, et al. Research Progress in Chemical Components, Pharmacological Effectiveness and Toxicity of Ferula assafoetid. Chinese Journal of Experimental Traditional Medical Formulae 2011;17:279-81.
18. Lin J, Jin M, Wu C, et al. Advances in studies on chemical constituents and pharmacological effects of Ferula. Strait Pharmaceutical Journal 2014;(5):1-3.
19. Daina A, Michielin O, Zoete V. SwissADME: a free web tool to evaluate pharmacokinetics, drug-likeness and medicinal chemistry friendliness of small molecules. Sci Rep 2017;7:42717.
20. Liu X, Ouyang S, Yu B, et al. PharmMapper server: a web server for potential drug target identification using pharmacophore mapping approach. Nucleic Acids Res 2010;38:W609-14.
21. UniProt: the universal protein knowledgebase. Nucleic Acids Res 2017;45:D158-69.
22. Stelzer G, Rosen N, Plaschkes I, et al. The GeneCards Suite: From Gene Data Mining to Disease Genome Sequence Analyses. Curr Protoc Bioinformatics 2016;54:1.30.1-1.30.33.
23. Shannon P, Markiel A, Ozier O, et al. Cytoscape: a software environment for integrated models of biomolecular interaction networks. Genome Res 2003;13:2498-504.
24. Szklarczyk D, Morris JH, Cook H, et al. The STRING database in 2017: quality-controlled protein-protein association networks, made broadly accessible. Nucleic Acids Res 2017;45:D362-8.
25. Tang Z, Li C, Kang B, et al. GEPIA: a web server for cancer and normal gene expression profiling and interactive analyses. Nucleic Acids Res 2017;45:W98-W102.
26. Chandrashekar DS, Bashel B, Balasubramanya SAH, et al. UALCAN: A Portal for Facilitating Tumor Subgroup Gene Expression and Survival Analyses. Neoplasia 2017;19:649-58.
27. Thul PJ, Lindskog C. The human protein atlas: A spatial map of the human proteome. Protein Sci 2018;27:233-44.
28. Zhang R, Li R, Zhang Y, et al. Immunohistochemical identification and fertility assessment of a mouse model of thin endometrium. Chinese Journal of Comparative Medicine 2018;28:19-26.
29. Szász AM, Lánczky A, Nagy Á, et al. Cross-validation of survival associated biomarkers in gastric cancer using transcriptomic data of 1,065 patients. Oncotarget 2016;7:49322-33.
30. Berman HM, Westbrook J, Feng Z, et al. The Protein Data Bank. Nucleic Acids Res 2000;28:235-42.
31. Trott O, Olson AJ. AutoDock Vina: improving the speed and accuracy of docking with a new scoring function, efficient optimization, and multithreading. J Comput Chem 2010;31:455-61.
32. Yu JW, Yuan HW, Bao LD, et al. Interaction between piperine and genes associated with sciatica and its mechanism based on molecular docking technology and network pharmacology. Mol Divers 2021;25:233-48.
33. Kasaian J, Mohammadi A. Biological activities of farnesiferol C: a review. J Asian Nat Prod Res 2018;20:27-35.
34. Kasaian J, Mosaffa F, Behravan J, et al. Modulation of Multidrug Resistance Protein 2 Efflux in the Cisplatin Resistance Human Ovarian Carcinoma Cells A2780/RCIS by Sesquiterpene Coumarins. Phytother Res 2016;30:84-9.
35. Kasaian J, Mosaffa F, Behravan J, et al. Reversal of P-glycoprotein-mediated multidrug resistance in MCF-7/Adr cancer cells by sesquiterpene coumarins. Fitoterapia 2015;103:149-54.
36. Hasanzadeh D, Mahdavi M, Dehghan G, et al. Farnesiferol C induces cell cycle arrest and apoptosis mediated by oxidative stress in MCF-7 cell line. Toxicol Rep 2017;4:420-6.
37. Li G, Li X, Cao L, et al. Sesquiterpene coumarins from seeds of Ferula sinkiangensis. Fitoterapia 2015;103:222-6.
38. Kamoldinov K, Li J, Eshbakova K, et al. Sesquiterpene coumarins from Ferula samarkandica Korovin and their bioactivity. Phytochemistry 2021;187:112705.
39. Jung JH, Kim MJ, Lee H, et al. Farnesiferol c induces apoptosis via regulation of L11 and c-Myc with combinational potential with anticancer drugs in non-small-cell lung cancers. Sci Rep 2016;6:26844.
40. Zhao L, Li J. Hypoxia adaption in life——An analysis of Nobel Prize in Physiology or Medicine in 2019. Science & Technology Review 2020;38:79-85.
41. Li L, Hou Z. MiR-125B-5p in Ovarian Cancer Tissue Reduces Tumor Energy Metabolism and Inhibits Tumor Cell Proliferation by Regulating Hexokinase-2. Chinese Journal of Cancer 2021;40:394-403.
42. He L, Lv S, Ma X, et al. ErbB2 promotes breast cancer metastatic potential via HSF1/LDHA axis-mediated glycolysis. Med Oncol 2022;39:45.
43. Patra KC, Hay N. The pentose phosphate pathway and cancer. Trends Biochem Sci 2014;39:347-54.
44. Jiang P, Du W, Wu M. Regulation of the pentose phosphate pathway in cancer. Protein Cell 2014;5:592-602.
45. Qin Z, Xiang C, Zhong F, et al. Transketolase (TKT)

activity and nuclear localization promote hepatocellular carcinoma in a metabolic and a non-metabolic manner. J Exp Clin Cancer Res 2019;38:154.
46. Li M, Zhao X, Yong H, et al. Transketolase promotes colorectal cancer metastasis through regulating AKT phosphorylation. Cell Death Dis 2022;13:99.
47. Li Y, Liu F, Pang B, et al. Discussion on Staged Intervention of Chronic Colitis-Cancer Transformation with the Method of Reinforcing Healthy Qi and Resolving Toxins: from the Perspective of Tumor Energy Metabolism Imbalance. Journal of Traditional Chinese Medicine 2022;63:234-9.

Cite this article as: Wang D, Sun Y, Liu Q, Ye C, Zhao S, Zhang H. *Ferula sinkiangensis* against gastric cancer: a network pharmacology, molecular docking and cell experiment study. Transl Cancer Res 2023;12(4):743-764. doi: 10.21037/tcr-22-2292

